Ocean Sci. Discuss., 12, 1669–1692, 2015
www.ocean-sci-discuss.net/12/1669/2015/
doi:10.5194/osd-12-1669-2015

Ocean Science
Discussions
Open Access

High resolution satellite turbidity and sea surface temperature observations of river plume interactions during a significant flood event

V. E. Brando[1,2], F. Braga[3], L. Zaggia[3], C. Giardino[1], M. Bresciani[1], D. Bellafiore[3], C. Ferrarin[3], F. Maicu[3], A. Benetazzo[3], D. Bonaldo[3], F. M. Falcieri[3], A. Coluccelli[4], A. Russo[4,5], and S. Carniel[3]

[1]Consiglio Nazionale delle Ricerche – Istituto per il Rilevamento Elettromagnetico Ambientale (CNR-IREA), Via Bassini 13, 20133 Milano, Italy
[2]Commonwealth Scientific & Industrial Research Organization (CSIRO), Canberra, Australia
[3]Consiglio Nazionale delle Ricerche – Istituto di Scienze Marine (CNR-ISMAR), Arsenale-Tesa 104, Castello 2737/F, 30122 Venezia, Italy
[4]Università Politecnica delle Marche – Dipartimento di Scienze della Vita e dell'Ambiente (UNIVPM-DISVA), Via Brecce Bianche, 60131 Ancona, Italy
[5]NATO STO Centre for Maritime Research and Technology, V.le San Bartolomeo 400, 19126 La Spezia, Italy

Received: 30 June 2015 – Accepted: 8 July 2015 – Published: 4 August 2015

Correspondence to: V. E. Brando (brando.v@irea.cnr.it)

Published by Copernicus Publications on behalf of the European Geosciences Union.

Abstract

Sea surface temperature (SST) and turbidity (T) derived from Landsat-8 (L8) imagery were used to characterize river plumes in the Northern Adriatic Sea (NAS) during a significant flood event in November 2014. Sea surface salinity (SSS) from an operational coupled ocean-wave model supported the interpretation of the plumes interaction with the receiving waters and among them.

There was a good agreement of the SSS, T, and SST fields at the sub-mesoscale and mesoscale delineation of the major river plumes. L8 30 m resolution enabled also the description of smaller plume structures.

Sharp fronts in T and SST delimited each single river plume. The isotherms and turbidity isolines coupling varied among the plumes due to differences in particle loads and surface temperatures in the discharged waters. The different plumes reflectance spectra were related to the lithological fingerprint of the sediments in the river catchments.

1 Introduction

Riverine discharges in the coastal ocean form river plumes, distinct regions where water masses properties are significantly influenced by riverine freshwater as it merges with deeper, salty and dynamical ocean waters (Horner-Devine et al., 2015). The extent, motion, and general structure of river plumes are mainly determined by the horizontal advection of freshwater from the river mouth, while the along-coast transport of the river-borne material is determined by several processes, including stratified-shear mixing, frontal processes, oceanic transport, tide and wind forcing, as well as Coriolis effects (Hetland, 2005; Horner-Devine et al., 2015). The relative importance of the mixing and transport processes determines the overall fate and transport of the freshwater discharge, as well as the dissolved and particulate matter concentrations within the plume (Horner-Devine et al., 2015).

Within the Mediterranean Sea, the Northern Adriatic Sea (NAS, Fig. 1) is the sub-basin most influenced by river plumes (DeGobbis et al., 2000; Spillman et al., 2007; Falcieri et al., 2014). The NAS is a shallow (average depth is smaller than 35 m) and semi-enclosed regional sea, which due to the high amount of freshwater is generally considered a dilution basin (DeGobbis et al., 2000; Spillman et al., 2007). The Po, Adige and Brenta rivers produce an almost single river plume, contributing 84 % of the total freshwater discharge delivered to the basin (Cozzi and Giani, 2011; Falcieri et al., 2014). However, the local effects of minor rivers should not be neglected, since they can contribute with low-salinity patches that are relevant to mesoscale and sub-mesoscale dynamics (Marini et al., 2008; Solidoro et al., 2009). These elevated freshwater discharges and associated particulate and dissolved matter inputs have a significant effect both on the physical and biogeochemical properties of the whole basin (Zavatarelli et al., 1998; Marini et al., 2008; Solidoro et al., 2009).

Following a large regional precipitation event affecting northern Italy, in November 2014 all NAS rivers area flooded concurrently (Fig. 2). Peak discharge for the Po River reached 8375 $m^3 s^{-1}$ on 19 November 2014, the fifth highest of the last hundred years (Montanari, 2012). The timing of the flood for each river varied reflecting the space–time distribution of precipitation and catchment morphology: Piave, Brenta and Isonzo peaked earlier on 6–7 November, Livenza and Adige on 8 November, while Po peaked the first time on 9 November ($\sim$ 4000 $m^3 s^{-1}$) and then reached the maximum discharge on 19 November. During this combined flood event a total of $\sim$ 15 km^3 of freshwater entered NAS, of which $\sim$ 10 km^3 entered the basin by 19 November, equating to $\sim$ 1 % of the basin volume.

Earth observation has been widely used to describe mesoscale dynamics and physical oceanographic characteristics of river plumes fronts using SST (sea surface temperature) and OCR (ocean colour radiometry) sensors (e.g. Ullman and Cornillon, 1999; D’Sa et al., 2007; Palacios et al., 2009; Schroeder et al., 2012). Several studies have combined SST with OCR data and/or with model data to quantify the extent, strength and variability of the river plumes fronts and to explain their behaviour in rela-

OSD
12, 1669–1692, 2015

tion to the main physical forcing processes (e.g. Hickey et al., 2005; Otero et al., 2009; Pietrzak et al., 2011; Falcini et al., 2012; Margvelashvili et al., 2013).

The recently launched Landsat-8 (L8 hereafter) has been deemed suitable for studying aquatic environments due to improved data quality and spectral coverage (Irons et al., 2012; Pahlevan et al., 2014). In this study we will combine SST and turbidity derived from L8 imagery to describe at fine spatial resolution (30 m) river plumes and their sub-mesoscale interactions in the NAS during the significant combined flood event of November 2014. To this aim we will also use the model data from an operational coupled ocean-wave modelling system to support the interpretation of the plume dynamic and their interaction with the receiving waters and among them.

2 Methods

2.1 Satellite imagery

To image the Earth throughout the visible and thermal portions of the spectrum, L8 carries two separate sensors, the Operational Land Imager (OLI) and the Thermal Infrared Radiometer Suite (TIRS). Both OLI and TIRS represent an evolution in Landsat sensor technology in terms of data quality and spectral coverage (Irons et al., 2012). The OLI provides coverage of the VNIR and SWIR portions of the spectrum at 30 m spatial resolution in nine spectral bands with a relatively high SNR (~ 300 for the blue bands) (Irons et al., 2012; Pahlevan et al., 2014). The TIRS adds two long-wave thermal spectral bands at 100 m spatial resolution, centred at 10.9 and 12.0 µm (bands 10 and 11, respectively) (Irons et al., 2012). Historically Landsat data has been used in coastal and inland waters to map both particulate matter and surface temperature (see Hellweger et al., 2004). OLI is considered particularly adequate for ocean colour retrievals and turbidity mapping due to its radiometric resolution and calibration accuracy (Pahlevan et al., 2014; Vanhellemont and Ruddick, 2014; Franz et al., 2015).

OSD
12, 1669–1692, 2015

In this study we used OLI and TIRS imagery of 19 November 2014 capturing a significant freshwater inflow into the NAS for mapping both turbidity and SST. For turbidity, OLI data were converted into water-leaving radiance reflectance (ρ_w, dimensionless) with ACOLITE, an automatic method for atmospheric correction designed specifically for OLI over turbid waters (Vanhellemont and Ruddick, 2014, 2015). The ρ_w data were then converted into turbidity (T) expressed in Formazin Nephelometric Unit (FNU) following Dogliotti et al. (2015). As at higher turbidity values, ρ_w (655 nm) starts to saturate while ρ_w (865 nm) still linearly increases with turbidity, they use a switching scheme to avoid saturation at 655 nm and retrieve accurately turbidity in the 1–1500 FNU range (Dogliotti et al., 2015). SST values were retrieved from atmosphere brightness temperature in TIRS band 10 with a radiative-transfer based atmospheric correction (Barsi et al., 2014, 2005).

2.2 Hydrodynamic forecasting model data

As a complement to the L8 images, we analysed model data generated by an operational implementation in the northern Adriatic basin of the Coupled Ocean–Atmosphere-Wave-Sediment Transport (COAWST, Warner et al., 2008) where the Regional Ocean Modeling System (ROMS) and the Simulating Wave Nearshore (SWAN) model are 2-way fully coupled (Russo et al., 2013a, b). COAWST was implemented for the NAS on a grid with horizontal spacing of 0.5 km and 12 vertical terrain-following *s*-levels, offline nested to parent operational models covering the whole Adriatic and the Italian seas ran by ARPA Emilia Romagna in Bologna (Italy) (Russo et al., 2013a, b). The operational system is forced by the operational high-resolution (7 km × 7 km) meteorological model COSMO-I7 (Russo et al., 2013a, b). Following Hetland (2005), at the river mouths grid cells momentum was injected giving a vertical structure to the plume, i.e. injecting most of the freshwater discharge in the surface layers (~ 80 % in the four uppermost sigma levels, corresponding to about 1.5 m). Daily time series of freshwater supplies from the Po river were imposed (and kept constant along the 72 h of forecast), while the remaining NAS rivers were prescribed based on monthly clima-

OSD
12, 1669–1692, 2015

Title Page
Abstract | Introduction
Conclusions | References
Tables | Figures
◂◂ | ▸▸
◂ | ▸
Back | Close
Full Screen / Esc
Printer-friendly Version
Interactive Discussion

tological estimates (Raicich, 1994). In order to represent the Po river delta system, the outflow measured at Pontelagoscuro (50 km upstream the river mouth) is split into five major branches (Maistra, Pila, Tolle, Gnocca and Goro) following the percentage division proposed in Zasso and Settin (2012). Minor Po river branches, north of the Po di Pila mouth, and some minor freshwater inputs (e.g. nearby the Caorle and Baseleghe wetlands) are not considered.

To delineate the surface extent of river plumes and the freshwater influence in the basin, the daily averaged surface level of the modelled salinity field was considered as the sea surface salinity (SSS). This approach explicitly does not consider the vertical structure of the plume or the mixed layer depth (as proposed in Otero et al., 2008, 2009) as the shallow waters of NAS and the weak tidal dynamics not always allow the development or the identification of a mixed layer (Falcieri et al., 2014).

3 Results and discussion

In the pseudo-true colour composite of the OLI imagery of 19 November 2014 (Fig. 1) two very large regions of freshwater influence (ROFI, Simpson, 1997) are delineated in the NAS by the convolution of the plumes generated by the northern rivers from the Isonzo to the Piave and then by the western rivers i.e., the Brenta, Adige and Po. As the river mouths are close to each other, sharp fronts delineate the river plumes from the cyclonic coastal current transporting dissolved and particulate matter from upstream plumes. The area in front of the Venice Lagoon shows specific patterns generated by the interaction between the coastal current and local tidal dynamics at the lagoon inlets, enhanced by the presence of long artificial jetties (Bellafiore, 2010).

3.1 Meteo-oceanographic conditions

The basin was characterized by relatively calm conditions in the days before the image retrieval. Regional circulation patterns in the week from 12 to 19 November were

OSD
12, 1669–1692, 2015

initially dominated by along-shore coastal currents (daily-average up to 0.7 $m\,s^{-1}$ at the surface), followed by effect of increasing riverine inflow spreading offshore with strong vertical gradients in temperature and salinity. These patterns are consistent with the conditions recorded at the Acqua Alta Oceanographic Tower (AAOT) located about 15 km off the Venice Lagoon (Fig. 1). On 19 November the average wind speed was 4 $m\,s^{-1}$ and the sea state was characterized by a mean significant wave height smaller of 0.3 m. Oceanic currents were weak reaching a vertically integrated value of 0.1 $m\,s^{-1}$, and mostly directed southwestwardly.

3.2 Spectral properties

From a qualitative point of view, the plumes and the coastal waters in the NAS appear very different in color ranging from white to yellow/brown shades in the RGB composite (Fig. 1). Figure 3 presents reflectance spectra extracted from selected locations of interest in NAS: the spectra for the center of the basin have a peak at 443 and 482 nm typical of blue waters (ρ_w (482) ranging 0.01–0.03), while the AAOT, the Venice lagoon inlets (Chioggia, Malamocco and Lido) and Grado inlet of the Marano lagoon have a 562 nm peak typical of green waters (ρ_w (562) ranging 0.04–0.07). The waters flowing from the western Marano lagoon (Lignano inlet) and Caorle and Baseleghe wetlands have higher spectra and ρ_w values at 562 and 655 nm are very similar (ranging 0.10–0.12 and 0.08–0.12, respectively).

The river plumes spectra show a peak at 655 nm of whitish/yellow/brown waters (ρ_w (655) ranging 0.09–0.23). In particular, the Isonzo, Tagliamento and Piave river plumes appear as almost white in the true-color as they have high ρ_w at both 562 and 655 nm, while the Po, Brenta, Adige, Sile and Livenza river plumes appear in yellow/brown shades, as ρ_w (562) is lower, ranging 0.08–0.12. The Po river plumes show ρ_w (865) ranging 0.10–0.12, similarly to ρ_w (655), whilst for all other river plume spectra ρ_w (865) was lower than the ρ_w (655).

OSD
12, 1669–1692, 2015

The very high reflectances and the colours of eastern Alpine rivers (Isonzo, Tagliamento and Piave) plumes are related to carbonate-rich sediments, yielded by their prevailing Mesozoic limestone and dolomite catchments (Pigorini, 1968; Castellarin and Vai, 1982). The yellow/brown shades of other rivers are due to the lithological fingerprint of their sediments. The Adige River drains a metamorphic and porphyric catchment in North-eastern Alps (Dinelli and Lucchini, 1999). The Po River drains both the Alps and Northern Apennines, respectively characterized by metamorphic-intrusive rocks and terrigenous sequence (shales, calcareous, mudstones and sandstones) (Dinelli and Lucchini, 1999). The remaining minor rivers, including Venice and Marano lagoons tributaries, mostly drain terrains constituted by mixed river deposits of the floodplain (Piovan et al., 2010). A considerable fraction of the flux from wetland-lagoon systems, constituted by organic particulate and high dissolved matter, also contribute to the dark-brown colour.

3.3 SST and SSS fields

Following Falcieri et al. (2014), we can identify the surface extent of the freshwater influence in the NAS with the 36 isohaline resulting from the salinity fields obtained by the numerical model (Fig. 4). The freshwater discharged during the combined flood event extended 15 km offshore for the plumes generated by the northern rivers, 18 km in front of the Adige and Brenta rivers and more than 60 km in front of the Po River, consistently with the Falcieri et al. (2014) high discharge plume patterns. Overall, the waters delineated by the 36 isohaline were colder (∼ 12–17 °C) than the saltier part of the basin (SST > ∼ 18 °C). In particular, SST ranged between 12–15 °C for the river and lagoon plumes, and between 15–17 °C in the coastal current connecting the river plumes. The area in front of the Venice Lagoon was warmer than the neighbouring ROFIs (SST = 16–18 °C).

The over-imposed isohalines showed a good correspondence with the observed SST field in delineating the major river plumes (Isonzo Tagliamento, Brenta, Adige and Po rivers). As some minor freshwater inputs (e.g. the Caorle and Baseleghe wetlands) are not considered in the model, there were some areas of mismatch between the SST and SSS fields in the coastal region east of the Venice Lagoon.

In the SST field is possible to identify small near-shore trapped warm water (NTTW) parcels, which are warmer than the adjacent plumes and the coastal current, and more similar to the central part of the basin (SST ranging 17–19 °C). These NTTWs are located outside of the Marano lagoon (45.71° N, 13.23° E), between the Sile and Piave river plumes (45.49° N, 12.64° E) and to the south of the Po di Pila (44.88° N, 12.49° E). These features were also spectrally different than the neighbouring waters, showing a peak typical of green waters with ρ_w (562) ranging 0.09–0.12 (Fig. 3). The locations of these small features are not adequately captured by the model derived SSS, most likely due to resolution issues.

3.4 Turbidity fields

Figure 5 presents the maps of T for the Isonzo to the Piave ROFI (Fig. 5a) and the Brenta, Adige and Po river plumes ROFI (Fig. 5b). The Tagliamento river plume presented the highest turbidity values ($T > 1700$ FNU) close to the mouth, while the Po river mouths plumes ranged 600–800 FNU, and the turbidity nearby the other river mouths ranged 100–300 FNU. For the open waters outside the ROFIs T ranged 1–5 FNU, while in the cyclonic coastal gyre connecting the plumes it ranged 10–30. As the wind and wave re-suspension was negligible during this event, T can be interpreted as a measure of the suspended particle load transported by the plumes in the basin.

The sharp fronts delimiting each single river plume observed in Figs. 1 and 4 appear delineated both by T and SST even if the isotherms and turbidity isolines coupling varied among the plumes due to differences in particle loads and surface temperatures in the discharged waters (Fig. 5c). The T and SST coupling does not necessarily reflect the composition of the transported particulate matter, as the Adige and Isonzo rivers (∼ 13 °C, ∼ 100 FNU) or the Livenza and Brenta rivers (∼ 14.5 °C, ∼ 150 FNU) have similar coupling but transport different material sources as described in Sect. 3.3. The dilution of the riverine freshwater within the plumes for the T and SST fields indicates

OSD
12, 1669–1692, 2015

that both quantities acted as possible tracers for freshwater influence in this specific event, perhaps with the exception of the NTTWs where T ranged 10–50 FNU, up to one order of magnitude lower than the neighbouring plumes and significantly higher the open seawaters.

3.5 Plume morphologies

The river plume structures can be described in terms of dynamical regions characterized by different dominant processes (Horner-Devine et al., 2015). Based on the presence/absence of these regions, Horner-Devine et al. (2015) proposed a classification of six plumes morphologies (plumes A–F). Following this classification, in Figs. 1, 4 and 5 the surface expressions of these morphologies can be identified for the NAS plumes observed on 19 November 2014:

- The Isonzo, Tagliamento, Piave, Adige and Brenta rivers form "prototypical" plumes ("plume A"), comprising all dynamical regions: the initial jet-like plume expansion forms a bulge that then merges in the coastal current.
- The Livenza River jet-like plume merges in the coastal current without forming an anticyclonic eddy, probably because of the very long jetties, hence it may be classified as non rotational plume ("Plume B").
- The freshwater discharged in the western side of the Marano Lagoon form on the sea-side a wide estuary plumes type ("plume C"). In this case the tidal dynamics lead to have no clear near-field, a weak mid-field, and no bulge.
- The discharge from the Baseleghe wetland forms an "angled inflow" plume ("plume D"), showing no bulge, due to a significant component of alongshore momentum as the inflow is at a small angle to the coast.
- The Po River enters the NAS through a deltaic system, delivering freshwater via five main river channels. The Po River Delta plume is the "convolution" of 12

OSD
12, 1669–1692, 2015

plumes formed by each of the channel outlets interacting with each other ("plume E"). Plume dynamics for each single plume depends of river flow thrust and on behaviour of neighbouring plumes. The plumes at the mouth of the various branches carry similar concentration of particulate matter (T = 600–800 FNU, Fig. 5), even if they differ in proportion of freshwater discharge.

- The shallow characteristics of the whole NAS littoral zone allow the identification of wider coastal areas where several rivers contribute to a common hydrodynamic pattern. The interactions of the northern rivers plumes from the Isonzo to the Piave River and then of the western rivers – the Brenta, Adige and Po river plumes – form two distinct ROFIs ("Plume F") where the plume water has lost memory of the inflow momentum but is still distinct from the ambient receiving water. The offshore borders of these ROFIs can be identified by the 36 isohaline corresponding to the 5 FNU isoline and the 18 °C isotherm.

- The Venice Lagoon, as a specific transitional water body with scarce freshwater sources in its interiors, could not properly classified as a ROFI. Coastal circulation in front of the lagoon is dominated by tidal dynamics and the presence of jetties and breakwaters at the inlets is highly influencing the shaping of less salty water (but still not freshwater) tidal plumes (Bellafiore, 2010).

4 Conclusions

In this study, the combined use of high-resolution OCR and SST imagery enabled the identification of the dynamical regions at small scale and sub-mesoscale for all plume structures and their interactions in the NAS. The independent satellite observations of T and SST were used as tracers for the surface expression of the freshwater influence in this significant flood event. This was corroborated by the good agreement of the patterns in these fields with the modelled SSS field at the sub-mesoscale and mesoscale. Furthermore, the spatial resolution of the L8 imagery enabled the classification of the

NAS plumes of 19 November 2014 based on their morphology including the description of smaller plume structures and the NTTWs in NAS, whilst these features were not adequately resolved by the 500 m resolution of the SSS model data.

Although the event discussed in this study was captured with a sensor having a revisiting time of 16 days, we expect that with the recent launch of ESA's Sentinel 2A and the forthcoming launch of Sentinel 2B the temporal resolution will increase reaching almost those normally associated with OCR missions (Dickey, 2003; Hestir et al., 2015; Mouw et al., 2015). Combined with their radiometric resolution similar to OCR missions, these developments will thus offer an opportunity to also describe the temporal evolution of plume structures at the sub-mesoscale.

The observed optical complexity of NAS due to the variability in composition of the particulate matter may affect accuracy of the Dogliotti et al. (2015) algorithm for T retrievals. Hence future work is needed to characterize optical properties of particulate and dissolved matter delivered by each river in flood and non-flood conditions. This will also enable the parameterization of other OCR algorithms (e.g. Melin et al., 2011; Vantrepotte et al., 2012; Brando et al., 2012) to accurately retrieve chlorophyll and suspended matter concentrations in these complex coastal waters.

There are almost no studies on the flux of water and sediment flowing through distributary branches of a delta or adjacent rivers due to the complexity and cost associated with a simultaneous sampling effort at all branches or rivers (Syvitski et al., 2005). Moreover flood events are difficult to observe in situ, as with ship-based activities is seldom possible to reach river mouths while autonomous vehicles are not operating in shallow waters (Hetland, 2005; Devlin and Schaeffelke, 2009). On the other hand, observations from instrumented sites or coastal observatories such as AAOT provide detailed information on a large array of variables but do not provide a sufficient spatial coverage and may happen not be located favorably to observe events of interest (Dickey, 2003).

The potential of an integrated use of earth observation, numerical models, and in-situ observations for describing coastal dynamics has been progressively emphasized

OSD
12, 1669–1692, 2015

in recent years (e.g. Dickey, 2003; Staneva et al., 2009; Stanev et al., 2011). The adoption of triple-collocation algorithms will allow the intercalibration of quantities and properties retrieved from the different sources (Janssen et al., 2007 and references therein). Furthermore, the use of the independent data sets will enable the identification of the relevant time- and space-scales for the observed (and modelled) phenomena (Chang et al., 2002).

Acknowledgements. Landsat 8 data were downloaded from USGS. Freshwater discharge data was provided by ARPA Veneto, ARPA Emilia Romagna e Protezione Civile del Friuli Venezia Giulia. Model data for the operational systems (COSMO-I7, AdriaROMS 4.0 and SWAN ITALIA) were provided by ARPA Emilia Romagna.

This study was co-funded by the CNR RITMARE Flagship Project, the European Union (FP7-People Co-funding of Regional, National and International Programmes, GA n. 600407) and the Italian Space Agency (CLAM-PHYM project, contract n. I/015/11/0).

We are grateful to RBINS for making ACOLITE publicly and freely available. Constructive comments by Erin Hestir, Mark Dowell, Andrea Bergamasco and Mauro Sclavo improved earlier versions of the manuscript.

References

Barsi, J. A., Schott, J. R., Palluconi, F. D., and Hook, S. J.: Validation of a Web-Based Atmospheric Correction Tool for Single Thermal Band Instruments, Earth Observing Systems X, San Diego, CA, USA, August 2005.

Barsi, J. A., Schott, J. R., Hook, S. J., Raqueno, N. G., Markham, B. L., and Radocinski, R. G.: Landsat-8 Thermal Infrared Sensor (TIRS) vicarious radiometric calibration, Remote Sens., 6, 11607–11626, doi:10.3390/rs61111607, 2014.

Bellafiore, D. and Umgiesser, G.: Hydrodynamic coastal processes in the North Adriatic investigated with a 3D finite element mode, Ocean Dynam., 60, 255–273, doi:10.1007/s10236-009-0254-x, 2010.

Brando, V. E., Dekker, A. G., Park, Y. J., and Schroeder, T.: Adaptive semianalytical inversion of ocean color radiometry in optically complex waters, Appl. Optics, 51, 2808–2833, 2012.

OSD

12, 1669–1692, 2015

High resolution satellite observations of river plume interactions

V. E. Brando et al.

Castellarin, A. and Vai, G. B.: Guida alla Geologia del Sudalpino Centro-orientale, Guide Geologiche Regionali., Soc. Geol. Ital., Bologna, Italy, 1982.
Chang, G. C., Dickey, T. D., Schofield, O. M., Weidemann, A. D., Boss, E., Pegau, W. S., Moline, M. A., and Glenn, S. M.: Nearshore physical processes and bio-optical properties in the New York Bight, J. Geophys. Res., 107, 3133, doi:10.1029/2001JC001018, 2002.
Cozzi, S. and Giani, M.: River water and nutrient discharges in the Northern Adriatic Sea: current importance and long term changes, Cont. Shelf Res., 31, 1881–1893, doi:10.1016/j.csr.2011.08.010, 2011.
DeGobbis, D., Precali, R., Ivancic, I., Smodlaka, N., Fux, D., and Kveder, S.: Long-term changes in the northern Adriatic ecosystem related to anthropogenic eutrophication, Int. J. Environ. Poll., 13, 495–533, doi:10.1504/IJEP.2000.002332, 2000.
Devlin, M. J. and Schaeffelke, B.: Spatial extent of riverine flood plumes and exposure of marine ecosystems in the Tully coastal region, Great Barrier Reef, Mar. Freshwater Res., 60, 1109–1122, doi:10.1071/MF08343, 2009.
Dickey, T.: Emerging ocean observations for interdisciplinary data assimilation systems, J. Marine Syst., 40–41, 5–48, doi:10.1016/S0924-7963(03)00011-3, 2003.
Dinelli, E. and Lucchini, F.: Sediment supply to the Adriatic sea basin from the Italian rivers: geochemical features and environmental constraints, Giornale Geol., 61, 121–135, 1999.
Dogliotti, A., Ruddick, K., Nechad, B., Doxaran, D., and Knaeps, E.: A single algorithm to retrieve turbidity from remotely-sensed data in all coastal and estuarine waters., Remote Sens. Environ., 156, 157–168, doi:10.1016/j.rse.2014.09.020, 2015.
D'Sa, E. J., Miller, R., and McKee, B. A.: Suspended particulate matter dynamics in coastal waters from ocean color: application to the northern Gulf of Mexico, Geophys. Res. Lett., 34, L23611, doi:10.1029/2007GL031192, 2007.
Falcieri, F. M., Benetazzo, A., Sclavo, M., Russo, A., and Carniel, S.: Po River plume pattern variability investigated from model data, Cont. Shelf Res., 87, 84–95, doi:10.1016/j.csr.2013.11.001, 2014.
Falcini, F., Khan, N. S., Macelloni, L., Horton, B. P., Lutken, C. B., McKee, K. L., Santoleri, R., Colella, S., Li, C., Volpe, G., D'Emidio, M., Salusti, A., and Jerolmack, D. J.: Linking the historic 2011 Mississippi River flood to coastal wetland sedimentation, Nat. Geosci., 5, 803–807, doi:10.1038/ngeo1615, 2012.

OSD
12, 1669–1692, 2015

Franz, B. A., Bailey, S. W., Kuring, N., and Werdell, P. J.: Ocean color measurements with the Operational Land Imager on Landsat-8: implementation and evaluation in SeaDAS, J. Appl. Remote Sens., 9, 096070, doi:10.1117/1.JRS.9.096070, 2015.
Hellweger, F. L., Schlosser, P., Lall, U., and Weissel, J. K.: Use of satellite imagery for water quality studies in New York Harbor, Estuar. Coast. Shelf S., 61, 437–448, 2004.
Hestir, E. L., Brando, V. E., Bresciani, M., Giardino, C., Matta, E., Villa, P., and Dekker, A. G.: Measuring freshwater aquatic ecosystems: the need for a hyperspectral global mapping satellite mission, Remote Sens. Environ, doi:10.1016/j.rse.2015.05.023, 2015.
Hetland, R. D.: Relating river plume structure to vertical mixing, J. Phys. Oceanogr., 35, 1667–1688, doi:10.1175/JPO2774.1, 2005.
Hickey, B. M., Geier, S. L., Kachel, N. B., and MacFadyen, A.: A bi-directional river plume: the Columbia in summer, Cont. Shelf Res., 25, 1631–1656, doi:10.1016/j.csr.2005.04.010, 2005.
Horner-Devine, A. R., Hetland, R. D., and MacDonald, D. G.: Mixing and Transport in Coastal River Plumes, Annu. Rev. Fluid Mech, 47, 569–594, doi:10.1146/annurev-fluid-010313-141408, 2015.
Irons, J. R., Dwyer, J. L., and Barsi, J. A.: The next Landsat satellite: the Landsat Data Continuity Mission, Remote Sens. Environ., 122, 11–21, doi:10.1016/j.rse.2011.08.026, 2012.
Janssen, P. A. E. M., Abdalla, S., Hersbach, H., and Bidlot, J. R.: Error estimation of buoy, satellite, and model wave height data, J. Atmos. Ocean. Tech., 24, 1665–1677, doi:10.1175/JTECH2069.1, 2007.
Margvelashvili, N., Andrewartha, J., Herzfeld, M., Robson, B., and Brando, V. E.: Satellite data assimilation and estimation of a 3d coastal sediment transport model using error-subspace emulators, Environ. Modell. Softw., 40, 191–201, doi:10.1016/j.envsoft.2012.09.009, 2013.
Marini, M., Jones, B. H., Campanelli, A., Grilli, F., and Lee, C. M.: Seasonal variability and Po River plume influence on biochemical properties along western Adriatic coast, J. Geophys. Res-Oceans, 113, C05S90, doi:10.1029/2007JC004370, 2008.
Melin, F., Vantrepotte, V., Clerici, M., D'Alimonte, D., Zibordi, G., Berthon, J.-F., Canuti, E.: Multi-sensor satellite time series of optical properties and chlorophyll-a concentration in the Adriatic Sea, Prog. Oceanogr., 9, 229–244, doi:10.1016/j.pocean.2010.12.001, 2011.
Montanari, A.: Hydrology of the Po River: looking for changing patterns in river discharge, Hydrol. Earth Syst. Sci, 16, 3739–3747, doi:10.5194/hess-16-3739-2012, 2012.

Mouw, C. B., Greb, S., Aurin, D., DiGiacomo, P. M., Lee, Z., Twardowski, M., Binding, C., Hu, C., Ma, R., Moore, T., Moses, W., and Craig, S. E.: Aquatic color radiometry remote sensing of coastal and inland waters: challenges and recommendations for future satellite missions, Remote Sens. Environ., 160, 15–30, doi:10.1016/j.rse.2015.02.001, 2015.

Otero, P., Ruiz-Villarreal, M., and Peliz, Á.: Variability of river plumes off North- west Iberia in response to wind events, J. Marine Syst., 72, 238–255, doi:10.1016/j.jmarsys.2007.05.016, 2008.

Otero, P., Ruiz-Villarreal, M., and Peliz, Á.: River plume fronts off NW Iberia from satellite observations and model data., J. of Mar. Sci., 66, 1853–1864, doi:10.1093/icesjms/fsp156, 2009.

Pahlevan, N., Lee, Z., Wei, J., Schaaf, C. B., Schott, J. R., and Berk, A.: On-orbit radiometric characterization of OLI (Landsat-8) for applications in aquatic remote sensing, Remote Sens. Environ., 154, 272–284, doi:10.1016/j.rse.2014.08.001, 2014.

Palacios, S. L., Peterson, T. D., and Kudela, R. M.: Development of synthetic salinity from remote sensing for the Columbia River plume, J. Geophys. Res., doi:10.1029/2008JC004895, 2009.

Pietrzak, J. D., Boer, G. J. D., and Eleveld, M. A.: Mechanisms controlling the intra-annual mesoscale variability of SST and SPM in the southern North Sea, Cont. Shelf Res., 31, 594–610, doi:10.1016/j.csr.2010.12.014, 2011.

Pigorini, B.: Sources and dispersion of recent sediments of the Adriatic Sea, Mar. Geol., 3, 187–229, doi:10.1016/0025-3227(68)90031-5, 1968.

Piovan, S., Mozzi, P., and Stefani, C.: Bronze Age paleohydrography of the southern Venetian Plain, Geoarchaeology, 25, 6–35, doi:10.1002/gea.20300, 2010.

Raicich, F.: Note on the flowrates of the Adriatic rivers. Tech. Rep. RF 02/94, CNR Istituto Sperimentale Talassografico, Trieste, Italy, 8, 1994.

Russo, A., Coluccelli, A., Carniel, S., Benetazzo, A., Valentini, A., Paccagnella, T., Ravaioli, M., and Bortoluzzi, G.: Operational models hierarchy for short term marine predictions: the Adriatic Sea example, MTS/IEEE OCEANS, Bergen, 2013a.

Russo, A., Carniel, S., and Benetazzo, A.: Support for ICZM and MSP in the Adriatic Sea region., Sea Technol., 54, 27–35, 2013b.

Schroeder, T., Devlin, M. J., Brando, V. E., Dekker, A. G., Brodie, J. E., Clementson, L. A., and McKinna, L.: Inter-annual variability of wet season freshwater plume extent into the Great Barrier Reef lagoon based on satellite coastal ocean colour observations, Mar. Pollut. Bull., 65, 210–223, doi:10.1016/j.marpolbul.2012.02.022, 2012.

Simpson, J. H.: Physical processes in the ROFI regime, J. Marine Syst., 12, 3–15, doi:10.1016/S0924-7963(96)00085-1, 1997.
Solidoro, C., Bastianini, M., Bandelj, V., Codermatz, R., Cossarini, G., Canu, D. M., Ravagnan, E., Salon, S., and Trevisani, S.: Current state, scales of variability, and trends of biogeochemical properties in the northern Adriatic Sea, J. Geophys. Res-Oceans, 114, C07S91, doi:10.1029/2008JC004838, 2009.
Spillman, C. M., Imberger, J., Hamilton, D. P., Hipsey, M. R., and Romero, J. R.: Modelling the effects of Po River discharge, internal nutrient cycling and hydrodynamics on biogeochemistry of the northern Adriatic Sea, J. Marine Syst., 68, 167–200, doi:10.1016/j.jmarsys.2006.11.006, 2007.
Stanev, E. V., Schulz-Stellenfleth, J., Staneva, J., Grayek, S., Seemann, J., and Petersen, W.: Coastal observing and forecasting system for the German Bight – estimates of hydrophysical states, Ocean Sci., 7, 569–583, doi:10.5194/os-7-569-2011, 2011.
Staneva, J., Stanev, E. V., Wolff, J.-O., Badewien, T. H., Reuter, R., Flemming, B., Bartholoma, A., and Bolding, K.: Hydrodynamics and sediment dynamics in the German Bight. A focus on observations and numerical modeling in the East Frisian Wadden Sea, Cont. Shelf Res., 29, 302–319, doi:10.1016/j.csr.2008.01.006, 2009.
Syvitski, J. P., Kettner, A. J., Correggiari, A., and Nelson, B. W.: Distributary channels and their impact on sediment dispersal, Mar. Geol., 222, 75–94, doi:10.1016/j.margeo.2005.06.030, 2005.
Ullman, D. S. and Cornillon, P. C.: Satellite-derived sea surface temperature fronts on the continental shelf off the northeast US coast, J. Geophys. Res., 104C, 23459–23478, doi:10.1029/1999JC900133, 1999.
Vanhellemont, Q. and Ruddick, K.: Turbid wakes associated with offshore wind turbines observed with Landsat 8, Remote Sens. Environ., 145, 105–115, doi:10.1016/j.rse.2014.01.009, 2014.
Vanhellemont, Q. and Ruddick, K.: Advantages of high quality SWIR bands for ocean colour processing: examples from Landsat-8, Remote Sens. Environ, 161, 89–106, doi:10.1016/j.rse.2015.02.007, 2015.
Vantrepotte, V., Loisel, H., Dessailly, D., and Mériaux, X.: Optical classification of contrasted coastal waters, Remote Sens. Environ., 123, 306–323, doi:10.1016/j.rse.2012.03.004, 2012.

OSD
12, 1669–1692, 2015

Warner, J. C., Sherwood, C. R., Signell, R. P., Harris, C., and Arango, H. G.: Development of a three-dimensional, regional, coupled wave, current, and sediment-transport model, Comput. Geosci., 34, 1284–1306, doi:10.1016/j.cageo.2008.02.012, 2008.

Zasso, M. and Settin, T.: Sulla ripartizione delle portate del Po tra i vari rami e le bocche a mare del delta: esperienze storiche e nuove indagini all'anno 2011, Relazione n. 02/12, ARPAV Dipartimento Regionale Per La Sicurezza Del Territorio, Belluno, Italy, 47, 2012 (in Italian).

Zavatarelli, M., Raicich, F., Bregant, D., Russo, A., and Artegiani, A.: Climatological biogeochemical characteristics of the Adriatic Sea, J. Marine Syst., 18, 227–263, doi:10.1016/S0924-7963(98)00014-1, 1998.

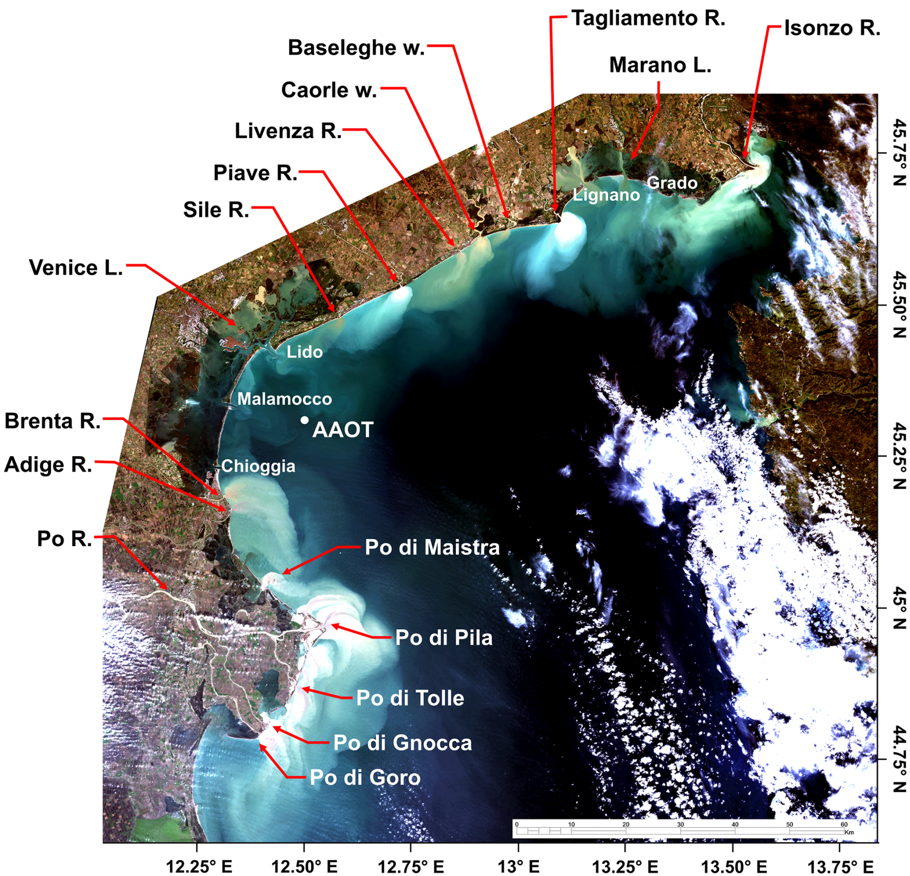

Figure 1. Study site. Pseudo true colour Landsat-8 OLI imagery acquired on 19 November 2014.

OSD
12, 1669–1692, 2015

High resolution satellite observations of river plume interactions

V. E. Brando et al.

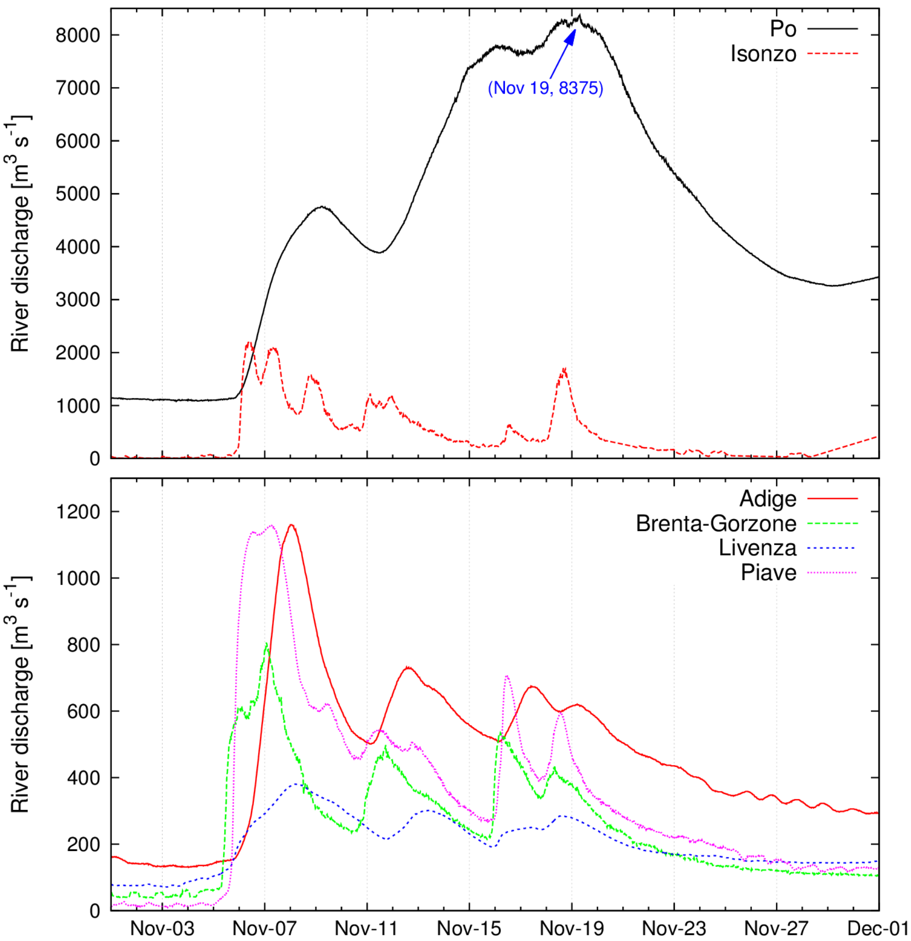

Figure 2. River discharge for November 2014 for the main rivers flowing in NAS.

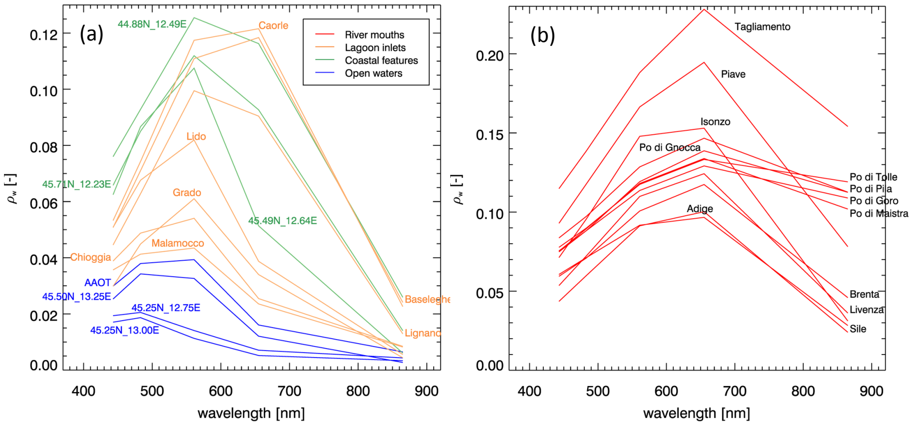

Figure 3. Reflectance spectra extracted from selected locations of interest in NAS, including open waters, coastal features, lagoon inlets **(a)**, and river mouths **(b)**.

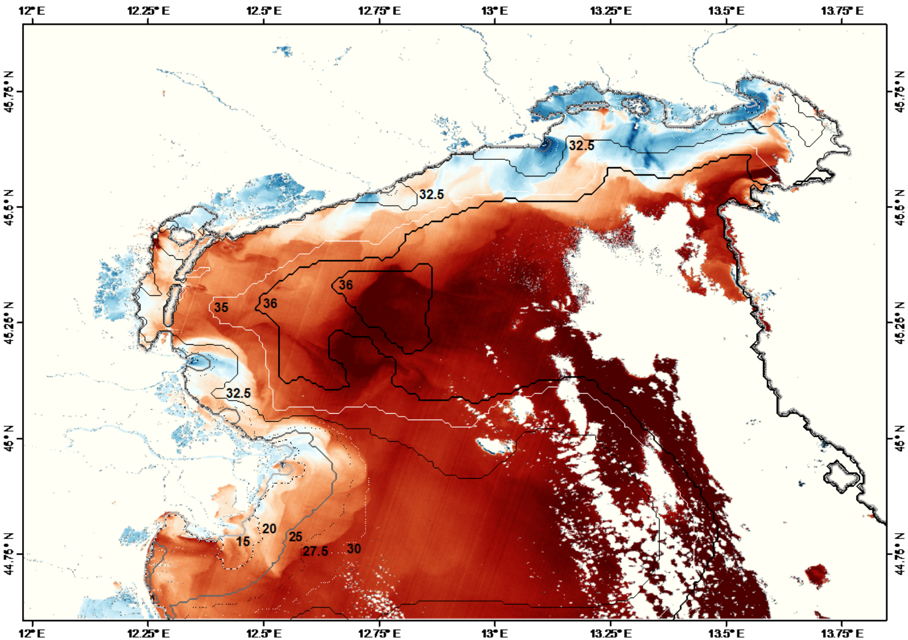

Figure 4. SST field estimated from Landsat-8 TIRS imagery acquired on 19 November 2014. Isohalines from the modelled SSS field are overlaid.

OSD
12, 1669–1692, 2015

High resolution satellite observations of river plume interactions

V. E. Brando et al.

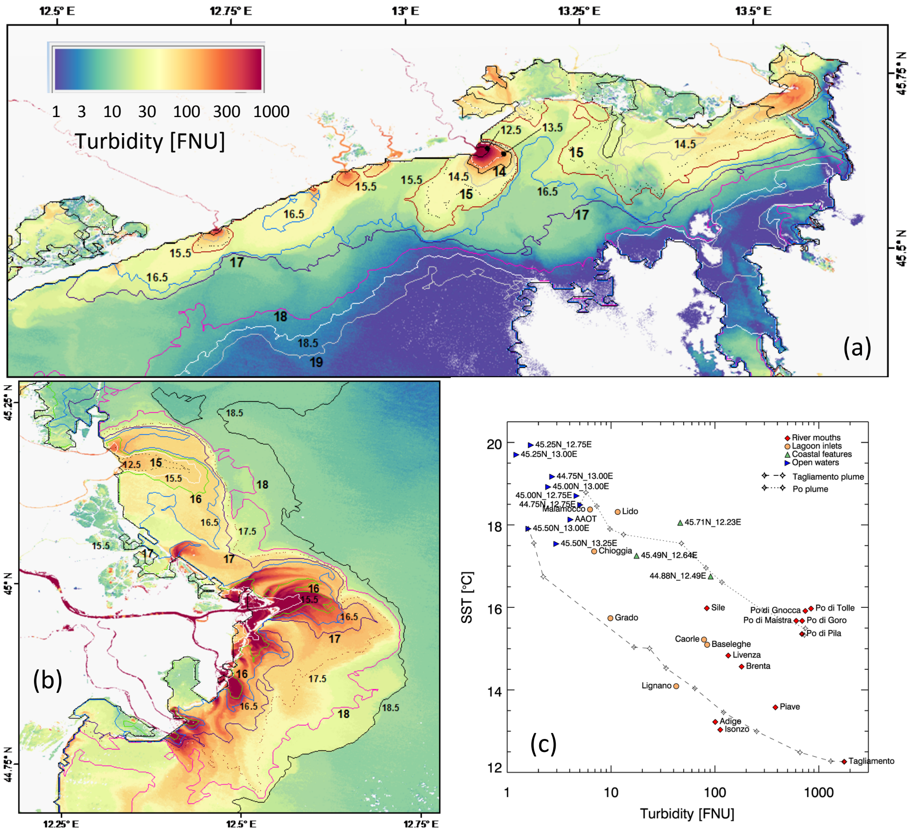

Figure 5. Turbidity map and SST isolines for **(a)** the cyclonic coastal current connecting all the plumes from the Isonzo to the Piave River, **(b)** the Brenta, Adige and Po river plumes **(c)** the Turbidity and SST values extracted at selected locations and the dilution of the Po and Tagliamento river plumes.

OSD
12, 1669–1692, 2015